

12-2019

## Characterization of the Dimerization Domains on the Mannose-6-phosphate/Insulin-like Growth Factor II Receptor

Tyler Degener  
tdegener@unomaha.edu

Follow this and additional works at: [https://digitalcommons.unomaha.edu/university\\_honors\\_program](https://digitalcommons.unomaha.edu/university_honors_program)

 Part of the [Biochemistry Commons](#), [Molecular Biology Commons](#), and the [Other Chemistry Commons](#)

---

### Recommended Citation

Degener, Tyler, "Characterization of the Dimerization Domains on the Mannose-6-phosphate/Insulin-like Growth Factor II Receptor" (2019). *Theses/Capstones/Creative Projects*. 82.  
[https://digitalcommons.unomaha.edu/university\\_honors\\_program/82](https://digitalcommons.unomaha.edu/university_honors_program/82)

This Dissertation/Thesis is brought to you for free and open access by the University Honors Program at DigitalCommons@UNO. It has been accepted for inclusion in Theses/Capstones/Creative Projects by an authorized administrator of DigitalCommons@UNO. For more information, please contact [unodigitalcommons@unomaha.edu](mailto:unodigitalcommons@unomaha.edu).



## CHARACTERIZATION OF THE DIMERIZATION DOMAINS ON THE MANNOSE-6-PHOSPHATE/INSULIN-LIKE GROWTH FACTOR II RECEPTOR

*Authors:*

Tyler Degener – tdegener@unomaha.edu  
Jodi Kreiling, PhD. – jkreiling@unomaha.edu

*Affiliation:*

Department of Chemistry  
University Honors Program  
University of Nebraska at Omaha

*In fulfillment of:*

HONR 4980 – Senior Honors Project/Thesis

### **ABSTRACT:**

The mannose-6-phosphate/insulin-like growth factor II (M6P/IGF2) receptor is a transmembrane protein known to sequester growth factors from the extracellular matrix. This behavior suggests a mechanism of tumor suppression. Structurally, the receptor's extracellular region is segmented into 15 homologous repeats, which are divided further into 5 triplet domains, labelled 1-3, 4-6, 7-9, 10-12, and 13-15. What is notable about the triplets is their propensity to form dimers with triplets on a second M6P/IGF2 receptor. In fact, previous studies indicate that this protein functions optimally when dimerized. Thus, the purpose of this experiment is to characterize these domain interactions. Using a urea and dithiothreitol (DTT) disruption assay, the 7-9 triplet's potential to dimerize was assessed. Preliminary results indicate that proximity is important for mediating interactions. The 7-9 triplet binds strongly to other 7-9 triplets on a separate M6P/IGF2 receptor; however, its association with any other triplet is not as strong comparatively.

### **KEYWORDS:**

Biochemistry, Endocrine Receptor, Tumor Suppression, Protein Oligomerization, Disruption Assay, Immunoblot

## **INTRODUCTION:**

### *Structure and Function of the M6P/IGF2 Receptor:*

The mannose-6-phosphate/insulin-like growth factor II (M6P/IGF2) receptor is a ubiquitous transmembrane protein linked to a host of cellular functions in vertebrates. Structurally, this approximately 300-kDa receptor features a small C-terminal intracellular tail, a transmembrane domain, and a large, N-terminal extracellular region<sup>1</sup>. This extracellular portion can be segmented into 15 homologous repeats, which fold into 5 triplet domains<sup>2</sup>. These triplets are approximately 50-75 kDa in size each, and can be labelled 1-3, 4-6, 7-9, 10-12, and 13-15 starting from the N-terminus. All repeats share a similar  $\beta$ -barrel architecture<sup>3</sup>, though their ligand binding affinities vary (Figure 1). The 10-12 triplet contains the principal insulin-like growth factor II (IGF2) binding site, while the 1-3 and 7-9 triplets contain the binding sites for mannosylated proteins (M6P proteins)<sup>4</sup>. The 4-6 triplet only weakly binds M6P proteins, while the 13-15 triplet is known to provide support between the full-length receptor's extracellular and transmembrane domains<sup>4</sup>.

In mammals, IGF2 is responsible for the promotion of cell growth—especially in developing fetuses<sup>2</sup>. Over-expression of this hormone is also responsible for the growth and division of various types of cancer cells<sup>5</sup>. From a mechanistic standpoint, IGF2 effects this change by downregulating apoptosis and upregulating cell proliferation<sup>6</sup>. Thankfully, the activity of IGF2 is regulated in part by the M6P/IGF2 receptor. This role therefore designates the receptor as a growth inhibitor/tumor suppressor<sup>2</sup>. In fact, loss-of-function mutations in the gene that codes for the M6P/IGF2 protein have been identified in a number of cancerous states<sup>7</sup>. The wild-type receptor is known to sequester IGF2 from the extracellular matrix and internalize it for degradation. The receptor-ligand complex is first targeted to a lysosome, where the IGF2 is released and destroyed<sup>5</sup>. Following this, the M6P/IGF2 receptor is recycled back to the surface of the cell once more<sup>8</sup>.

This receptor is also known to bind M6P proteins and direct them toward their final destination within the cell<sup>6</sup>. In disease states, this functionality can be severely impaired, which leads to insufficient breakdown of ligands within the lysosome<sup>9</sup>. The ability of the M6P/IGF2 receptor to bind its two primary ligands is thus imperative to maintaining the health of any given cell.

### *Rationale Behind the Current Experiment:*

It has been noted that the M6P/IGF2 receptor binds ligands best when it is dimerized with a second M6P/IGF2 receptor<sup>10-13</sup>; however, there is limited information as to how this interaction is mediated. Therefore, the purpose of this experiment is to characterize the way in which this receptor dimerizes. This investigation will be carried out at the level of the triplet domains. In other words, which triplets interact preferentially with one another? Such information could be used to further elucidate the full-length receptor's mechanism of tumor suppression.

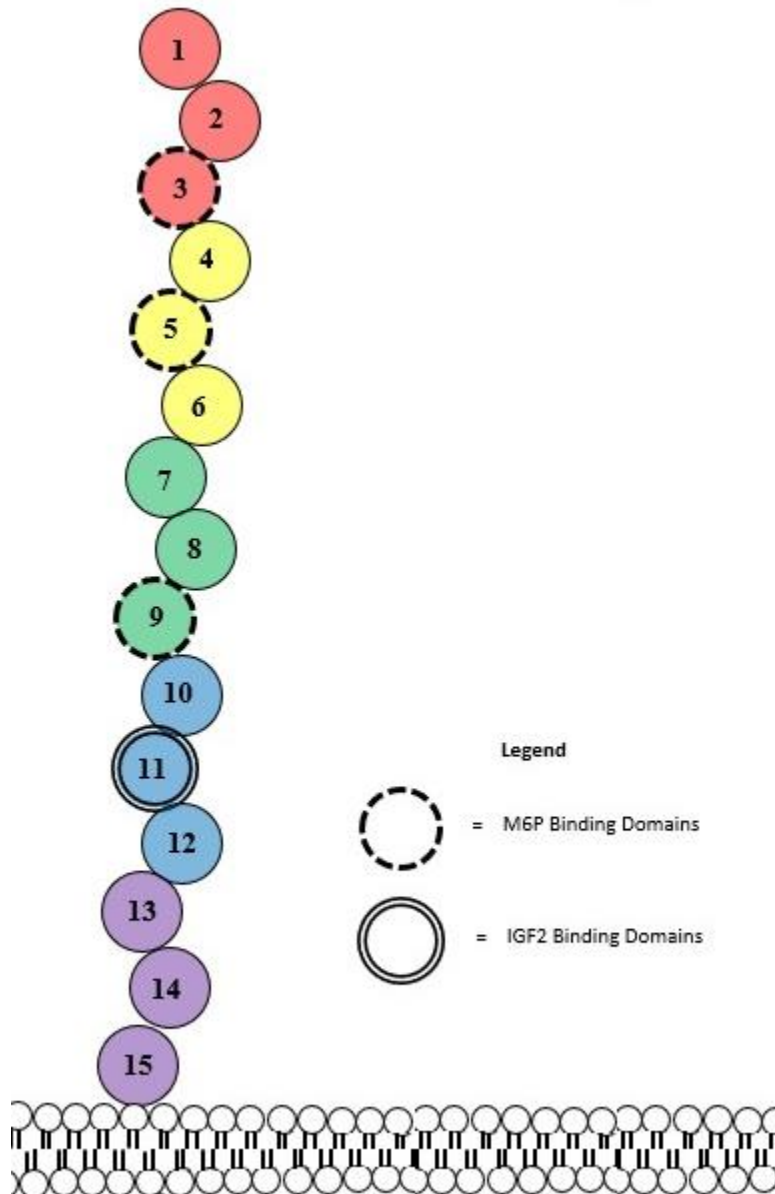
Undergraduates who have worked previously in Dr. Kreiling's laboratory have devised a method of expressing each triplet domain in isolation<sup>2</sup>. Many of these triplets were also tagged with molecular markers so that they could be visualized once probed with fluorescent antibodies. For instance, each of the five triplets have been marked with a FLAG (F) tag. A separate 7-9 construct has also been labelled with a MycHis (MH) tag.

Prior work in Dr. Kreiling's lab has also shown that the 7-9 triplet in particular has an affinity for each of the other triplet domains—including itself. The question stated above can thus be reformulated. Which of the triplet pairs form the strongest interactions? Two hypotheses can be

made regarding the dimerization of the triplets. One conjecture is that the strongest interactions will be between identical triplets (i.e. 7-9 and 7-9), which would imply that structure is the best predictor of dimerization. Another view is that the strongest interaction will be between triplets with similar functions (i.e. 7-9 and 1-3). The strength of the triplets' interactions can be gauged using a chemical disruption assay. Preliminary work suggests that a combination of urea and dithiothreitol (DTT) works best for such a procedure.

The purpose of this current experiment can thus be narrowed considerably. This work aims to quantitatively assess the strength of the dimers formed between the 7-9 triplet and every other triplet domain. The motivation behind this exercise is self-evident: characterizing the optimal binding of the triplets will be critical to understanding the receptor's role as a tumor suppressor.

**Figure 1. Structure of the Extracellular M6P/IGF2 Receptor**



A cartoon representation of the extracellular portion of the M6P/IGF2 receptor. The individual domains have been labelled 1-15, starting from the N-terminus. Triplet regions have been grouped together using a color code. The outline of each domain communicates which ligand it binds. These binding affinities depend on the receptor's ability to dimerize with a second M6P/IGF2 receptor on the surface of the same cell.

## **MATERIALS AND METHODS:**

### *DNA Purification:*

The genes coding for the 7-9MH triplet and all five of the F-tagged triplets had each been inserted into their own pCMV5 plasmid vector. Large-scale samples of this DNA were isolated using Qiagen's Plasmid Maxi Prep Kit. Following isolation, the DNA was reconstituted in de-ionized water. The concentration of the purified DNA was then assessed by reading the absorbance of the aqueous DNA solution at 260 nm using a standard UV-Vis spectrophotometer.

### *Cell Culture:*

Human embryonic kidney (HEK) 293 cells were incubated at 37 °C in a 5.0% carbon dioxide atmosphere. The cells were cultured with Dulbecco's Modified Eagle Medium (DMEM), which contained 5.0% bovine growth serum (BGS). A 1.5 mL aliquot of cells were passaged to a new flask with 18 mL of new HEK 293 Media approximately twice a week.

### *Cell Transfection:*

A modified calcium phosphate method was used to transfect the HEK 293 cells. Cells were split on the first day of the procedure at a ratio of 1:10 in refrigerated HEK 293 Media. Following an overnight incubation at 37 °C and 5.0% CO<sub>2</sub>, the cells were transfected on the second day. Four 100 mm plates were prepared for each of the following seven conditions. Five of the conditions had 7-9MH co-transfected with a F-tagged DNA construct: 1-3F, 4-6F, 7-9F, 10-12F, or 13-15F. The sixth condition had 7-9MH co-transfected with a blank pCMV5 vector. The seventh condition had 1-3F co-transfected with 7-9F. These final two pairings served as negative experimental controls.

Each of the DNA constructs described above were prepared in the following solution: 2025 µL of cell culture grade water, 297 µL of 2.0 M calcium chloride, and the appropriate volume of DNA needed to deliver 10 µg of DNA to each plate. This solution was added to 2250 µL of HBS (42 mM HEPES, 274 mM sodium chloride, 10 mM potassium chloride, 1.8 mM sodium phosphate dibasic, pH 7.40) with vortexing. This mixture was allowed to precipitate for 10 minutes on ice. A 1.0 mL aliquot of the appropriate mixture was then added to each plate. Following this, the cells were again incubated overnight at 37 °C and 5.0% CO<sub>2</sub>. On the third day of the procedure, the old cell media was aspirated off of the plates and replaced with fresh DMEM (containing no BGS).

### *Cell Lysis:*

When the cells were ready to be lysed, the media was aspirated off of each plate. The cells were then washed twice with HBS, being careful not to disrupt the cells. A third aliquot of HBS was delivered to each plate, after which the cells were scraped off. The cells from each condition mentioned above were then combined into a 15 mL tube and centrifuged for 3 minutes at 2000 rpm. The supernatant was discarded following this spin, leaving only a cell pellet. A 1.0 mL aliquot of Lysis Mix (1:100 phenylmethylsulfonyl fluoride, 1:500 protease inhibitor complex, in Extraction Buffer (10 mM HEPES, 1.0% Triton X-100, 1.0 mM magnesium chloride, pH 7.4)) was added to each cell pellet. The cells were incubated in the Lysis Mix for 1 hour, then centrifuged for 7 minutes at 13000 rpm. The supernatants, which contained the desired triplet proteins, were stored at -80 °C when not in use.

#### *Confirmation of Protein Expression:*

To confirm that the cells had expressed the triplet proteins, the lysates were separated via sodium dodecyl sulfate polyacrylamide gel electrophoresis (SDS-PAGE). Sample lysates were first dyed with Li-Cor's 4X Protein Loading Buffer (containing 1:10  $\beta$ -mercaptoethanol) and denatured via heat. Proteins were then separated on two identical SDS-PAGE gels (4-20% gradient). A Li-Cor Molecular Weight Marker ran alongside the lysates as a size reference. The gels were transferred to nitrocellulose membranes using Bio-Rad's Trans-Blot Turbo instrument (25 V, 2.5 A, 7 minutes).

Membranes were rinsed end-over-end with Odyssey Blocking Buffer for 1 hour at room temperature. One of the two membranes was then probed with an anti-His antibody (1:1000 in Odyssey Blocking Buffer) and the other with anti-FLAG antibody (1:1000 in Odyssey Blocking Buffer) overnight at 4 °C. Following this incubation with primary antibody, the membranes were washed end-over-end with 1X TBST (0.1% Tween 20, 100 mM Tris-HCl, 0.9% sodium chloride, pH 7.4) for 5 minutes, a total of three times each. Each membrane was then probed with Li-Cor's IRDye 680RD goat anti-mouse antibody (1:7000 in Odyssey Blocking Buffer) for 30 minutes. This was followed by a second round of rinses with 1X TBST. Protein bands were finally detected via near-infrared fluorescence imaging using a Li-Cor Odyssey Fc imaging system set to 700 nm.

#### *Confirmation of Dimerization Between 7-9MH and F-tagged Triplets:*

A nickel pull down assay was used to confirm that the 7-9 triplet formed dimers with every other triplet. A ThermoFisher Scientific Ni-NTA slurry was first vortexed, then 40  $\mu$ L were added to a microfuge tube. The slurry was centrifuged at 800 xg for 2 minutes, and afterward the supernatant was discarded. The remaining resin was next equilibrated with 40  $\mu$ L of Equilibration Buffer (20 mM sodium phosphate, 10 mM imidazole, 300 mM sodium chloride, pH 7.4) and again centrifuged. After removing the Equilibration Buffer, the following was added to the prepared nickel resin: 40  $\mu$ L of cell lysate, 40  $\mu$ L of Equilibration Buffer, and 80  $\mu$ L of de-ionized water. The resin was then allowed to rotate end-over-end overnight at 4 °C.

After equilibration with the sample lysates, the resin was centrifuged again at 800 xg for 2 minutes. The supernatant was discarded, and 80  $\mu$ L of Wash Buffer (20 mM sodium phosphate monobasic, 20 mM imidazole, 300 mM sodium chloride, pH 7.4) was added. Following this, the resin was centrifuged again as before. This wash procedure was done twice. Bound proteins were then eluted from the column by adding 10  $\mu$ L of Elution Buffer (20 mM sodium phosphate, 250 mM imidazole, 300 mM sodium chloride, pH 7.4) and centrifuging. The supernatant was then transferred to a clean microfuge tube. This elution procedure was done a total of three times to yield a final volume of 30  $\mu$ L. The eluted proteins were then separated via SDS-PAGE and visualized via immunoblot as described above.

#### *Dimer Disruption Assays:*

To assess the strength of the dimerization interactions observed between 7-9 and the other triplets, a urea and dithiothreitol (DTT) disruption assay was performed. The nickel pull down assay was modified slightly, such that 1.0 mL of an aqueous solution of urea (concentration variable) and DTT (5 mM) was added to the resin following equilibration with the lysate. The resin was then incubated end-over-end for 1 hour at room temperature. Following the disruption, the resin was centrifuged at 800 xg for 2 minutes, and the supernatant was discarded. Next, the resin was washed twice with 200  $\mu$ L of Wash Buffer, similar to above. The bound proteins were then eluted as before, separated via SDS-PAGE, and visualized via immunoblot.

## RESULTS:

### *Confirmation of Protein Expression:*

The transfection procedure yielded cell lysates which contained appreciable amounts of both 7-9MH and each of the F-tagged triplets (Figure 2). The only combination of proteins unable to be obtained was the 7-9MH/13-15F pair, which expressed rather poorly in the HEK 293 cells.

As expected, the pCMV5 vector (used as a negative control) did not fluoresce after treatment with either the anti-His or the anti-FLAG antibodies. As such, it can be concluded that these primary antibodies bind only to their intended molecular target—in this case, the H- or the F-tag respectively. Proteins lacking one of these specific tags are thus rendered invisible according to the method of immunoblotting described above.

### *Confirmation of Dimerization Between 7-9MH and F-tagged Triplets:*

For all triplet pairs (excluding 7-9MH/13-15F), the 7-9MH receptor and the F-tagged receptor were both present on the immunoblot following purification of the lysates with the Ni-NTA resin (Figure 3). This is notable because the Ni<sup>2+</sup> ion bound to the resin has a high affinity for polyhistidine regions, such as those comprising the MH-tag. The resin's manufacturer mentions no specific affinity for the F-tag, nor are there any internal polyhistidine regions in the primary sequence of the receptor itself.

Strangely however, the 1-3F/7-9F pair (intended for use as a negative control) shows up on the immunoblot as well. Since the nickel resin has no specific affinity for either of these proteins, neither one should appear here. The unexpected presence of 1-3F/7-9F most likely indicates that the receptors themselves, or the FLAG-tag, are non-specifically binding to the resin.

### *Dimer Disruption Assays:*

For each of the triplet pairs expressed prior, a disruption assay was performed. Each unique assay was then performed in triplicate to ensure reproducibility of results. The 7-9MH/pCMV5 pair was again used as a negative control (Figure 4). The blank vector was not expected to dimerize with 7-9MH, nor was it expected to fluoresce on the immunoblot. The results seen are consistent with both of these expectations.

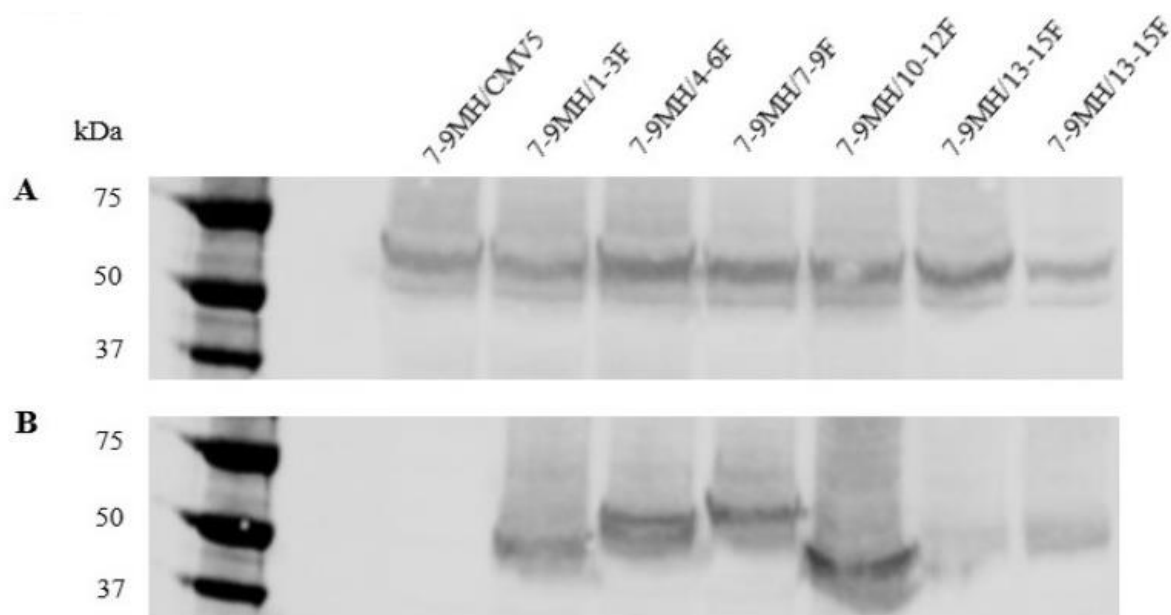
The incubation of each 7-9MH/triplet-F pair, while on the resin, with high concentrations of urea successfully disrupted the protein-protein interaction only when DTT was added additionally (Figures 5-8). These denaturants also had no visible effect on the nickel-histidine interaction, as evidenced by consistent band intensity across each 7-9MH panel. That said, as the concentration of urea was increased, so too did the intensity of the F-tagged bands diminish. This suggests that the triplet dimer was being split apart. The extent of this disruption was variable depending on which triplet pair was experimented with.

Critically, this disruption assay shows that—at a given concentration of urea—some triplets associate with 7-9 more strongly than others. This is evidenced by the variable intensity of the F-tagged bands as seen across the immunoblots. To quantify how much of the intact dimer remained after disruption, the intensity of the F-tagged band was measured relative to the 7-9MH band after treatment with 8.0 M urea and 5.0 mM DTT (Table 1). A higher percent dimerization thus indicates a stronger interaction between the given pair of triplets. Each disruption assay was done in triplicate, so the values presented below represent an average across three trials.

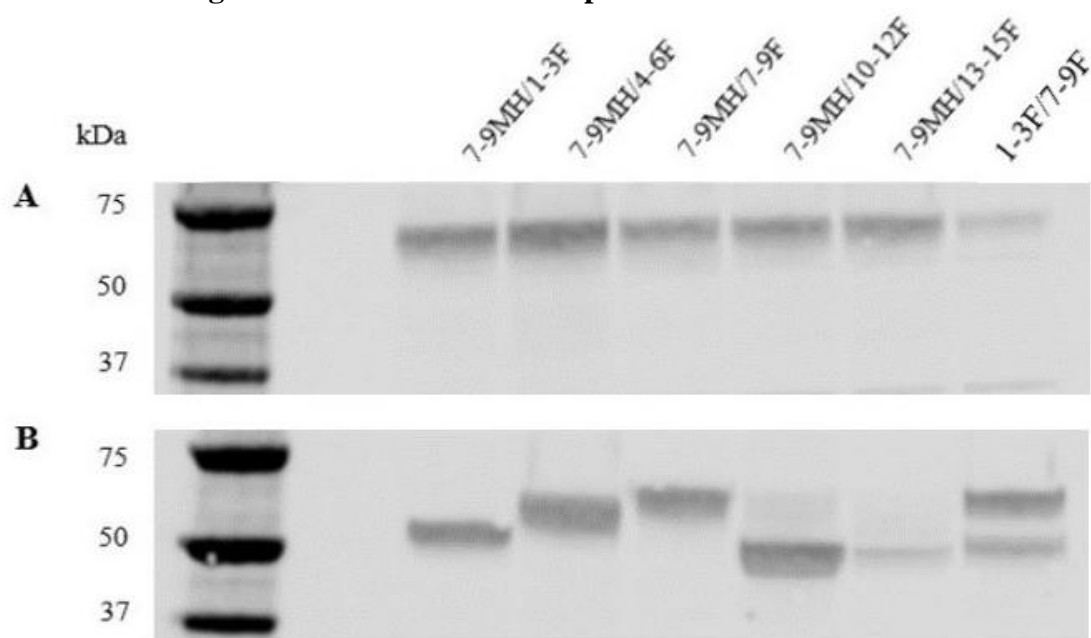


**Table 1. Extent of Dimerization After Disruption with 8.0 M Urea and 5.0 mM DTT**

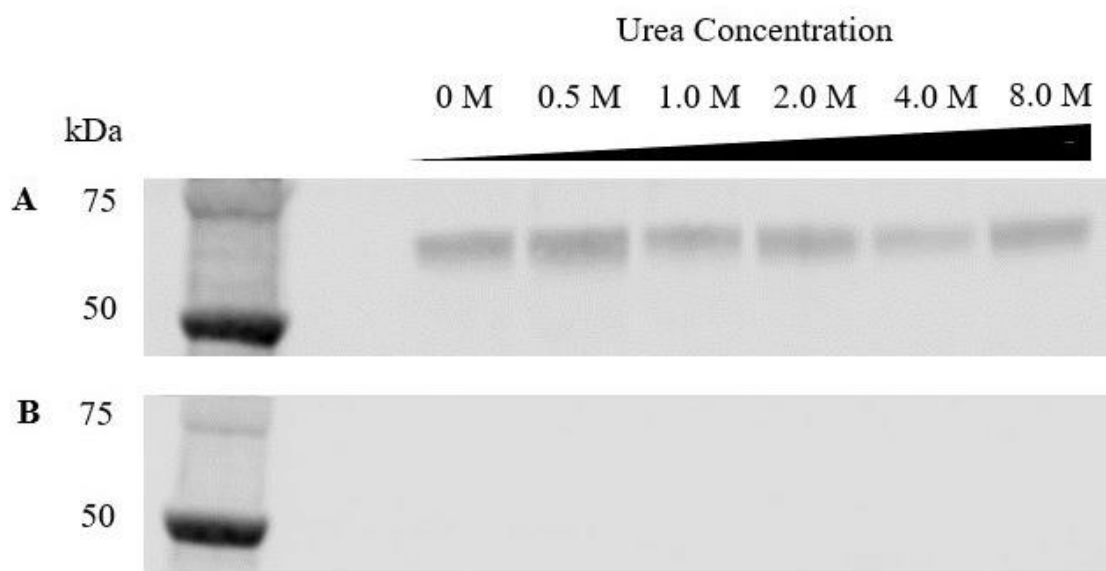
<i>Triplet Pair</i>	7-9MH/1-3F	7-9MH/4-6F	7-9MH/7-9F	7-9MH/10-12F
<i>Percent Dimerized</i>	17%	35%	41%	29%

**Figure 2. Confirmation of Triplet Protein Expression**

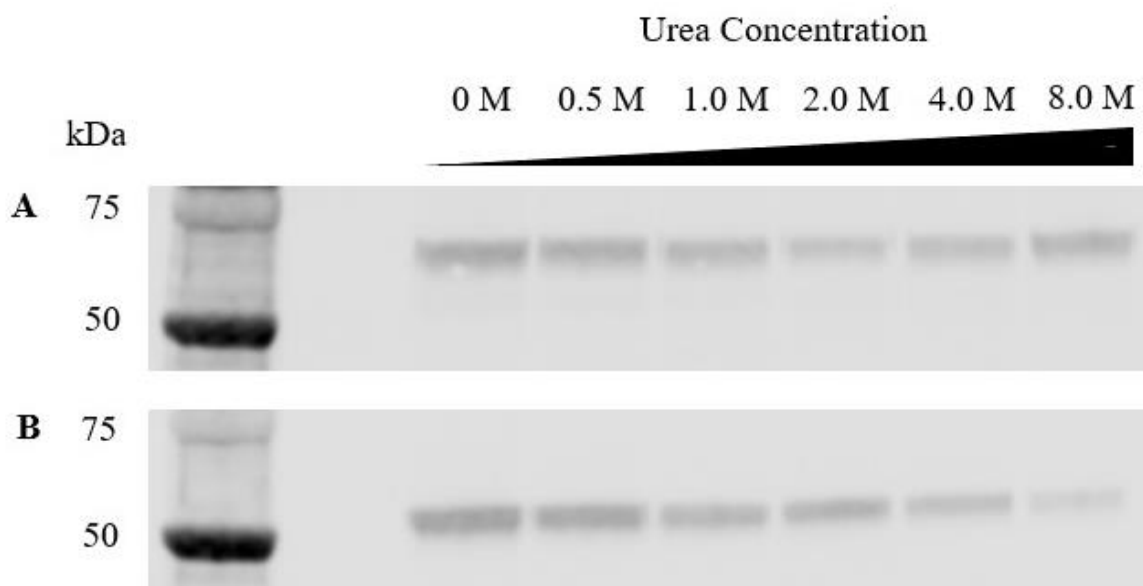
**A)** SDS-PAGE gel (4-20% gradient) transferred to a nitrocellulose membrane and immunoblotted with anti-His antibodies to confirm the expression of the 7-9MH triplet in the HEK-293 cell lysates. **B)** SDS-PAGE gel (4-20% gradient) transferred to a nitrocellulose membrane and immunoblotted with anti-FLAG antibodies to confirm the expression of the F-tagged triplets in the HEK-293 cell lysates. The pCMV5 vector functions as a negative control. Two different 7-9MH/13-15F lysates were blotted to assess which of two available 13-15F constructs expressed more protein.

**Figure 3. Confirmation of Triplet Protein Dimerization**

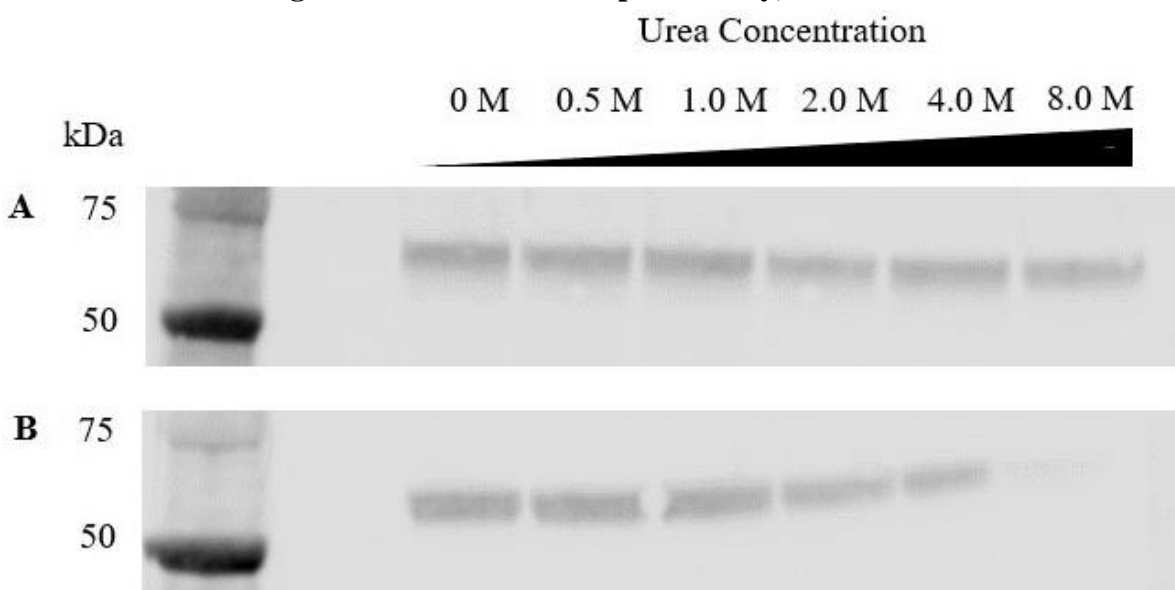
**A)** SDS-PAGE gel (4-20% gradient) transferred to a nitrocellulose membrane and immunoblotted with anti-His antibodies to confirm the presence of the 7-9MH triplet. **B)** SDS-PAGE gel (4-20% gradient) transferred to a nitrocellulose membrane and immunoblotted with anti-FLAG antibodies to confirm the presence of the F-tagged triplets. Triplet pairs were passed through, then eluted, from Ni-NTA chromatography resin before separation on the gel. The  $\text{Ni}^{2+}$  on the column has a high affinity for the MH-tag—and not the F-tag. Thus, the presence of any F-tagged proteins on the gel is indirect evidence of dimerization with the 7-9MH protein. The unexpected presence of the 1-3F/7-9F pair complicates this assessment, however.

**Figure 4. Urea/DTT Disruption Assay, 7-9MH/pCMV5**

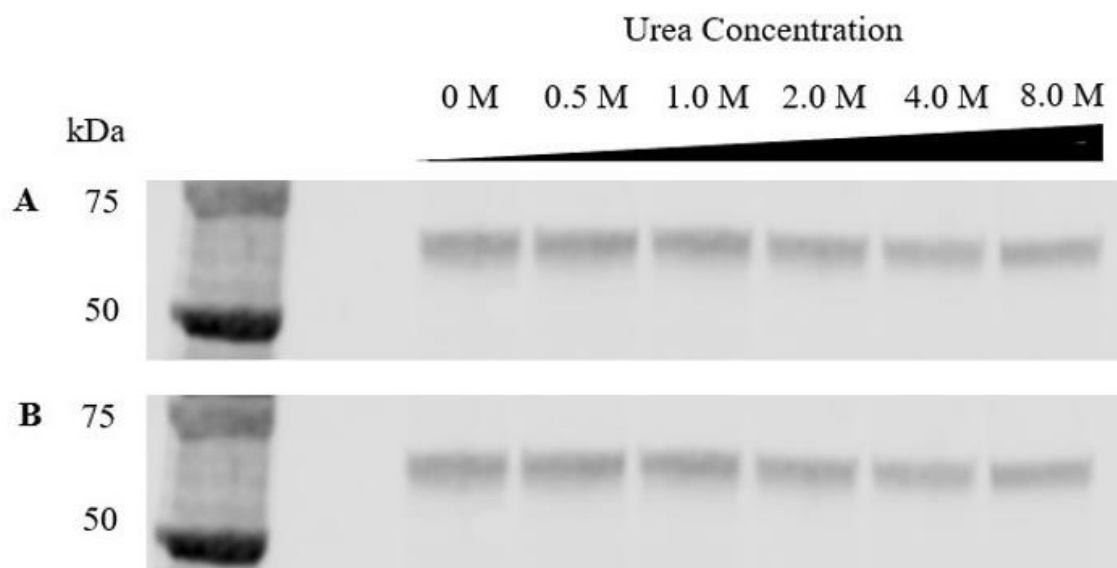
**A)** SDS-PAGE gel (4-20% gradient) transferred to a nitrocellulose membrane and immunoblotted with anti-His antibodies to confirm the presence of the 7-9MH triplet. **B)** SDS-PAGE gel (4-20% gradient) transferred to a nitrocellulose membrane and immunoblotted with anti-FLAG antibodies to confirm the presence of any F-tagged triplet. Triplet pairs were bound to a Ni-NTA chromatography column, then treated with 5.0 mM DTT and a variable concentration of urea. The proteins that remained on the column following a subsequent wash were eluted and then separated via gel. The pCMV5 vector was used as a negative control; thus, it is predictably absent from both immunoblots.

**Figure 5. Urea/DTT Disruption Assay, 7-9MH/1-3F**

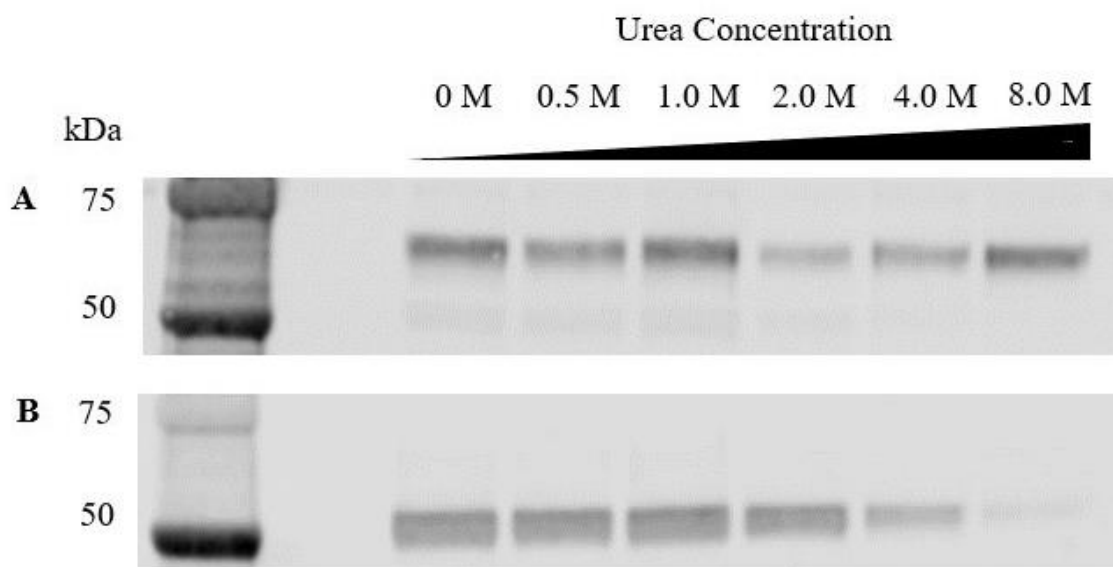
**A)** SDS-PAGE gel (4-20% gradient) transferred to a nitrocellulose membrane and immunoblotted with anti-His antibodies to confirm the presence of the 7-9MH triplet. **B)** SDS-PAGE gel (4-20% gradient) transferred to a nitrocellulose membrane and immunoblotted with anti-FLAG antibodies to confirm the presence of the 1-3F triplet. Triplet pairs were bound to a Ni-NTA chromatography column, then treated with 5.0 mM DTT and a variable concentration of urea. The proteins that remained on the column following a subsequent wash were eluted and then separated via gel. The intensity of the F-tagged band at high concentrations of urea is assumed to correlate positively with the strength of the dimer.

**Figure 6. Urea/DTT Disruption Assay, 7-9MH/4-6F**

**A)** SDS-PAGE gel (4-20% gradient) transferred to a nitrocellulose membrane and immunoblotted with anti-His antibodies to confirm the presence of the 7-9MH triplet. **B)** SDS-PAGE gel (4-20% gradient) transferred to a nitrocellulose membrane and immunoblotted with anti-FLAG antibodies to confirm the presence of the 4-6F triplet. Triplet pairs were bound to a Ni-NTA chromatography column, then treated with 5.0 mM DTT and a variable concentration of urea. The proteins that remained on the column following a subsequent wash were eluted and then separated via gel. The intensity of the F-tagged band at high concentrations of urea is assumed to correlate positively with the strength of the dimer.

**Figure 7. Urea/DTT Disruption Assay, 7-9MH/7-9F**

**A)** SDS-PAGE gel (4-20% gradient) transferred to a nitrocellulose membrane and immunoblotted with anti-His antibodies to confirm the presence of the 7-9MH triplet. **B)** SDS-PAGE gel (4-20% gradient) transferred to a nitrocellulose membrane and immunoblotted with anti-FLAG antibodies to confirm the presence of the 7-9F triplet. Triplet pairs were bound to a Ni-NTA chromatography column, then treated with 5.0 mM DTT and a variable concentration of urea. The proteins that remained on the column following a subsequent wash were eluted and then separated via gel. The intensity of the F-tagged band at high concentrations of urea is assumed to correlate positively with the strength of the dimer.

**Figure 8. Urea/DTT Disruption Assay, 7-9MH/10-12F**

**A)** SDS-PAGE gel (4-20% gradient) transferred to a nitrocellulose membrane and immunoblotted with anti-His antibodies to confirm the presence of the 7-9MH triplet. **B)** SDS-PAGE gel (4-20% gradient) transferred to a nitrocellulose membrane and immunoblotted with anti-FLAG antibodies to confirm the presence of the 10-12F triplet. Triplet pairs were bound to a Ni-NTA chromatography column, then treated with 5.0 mM DTT and a variable concentration of urea. The proteins that remained on the column following a subsequent wash were eluted and then separated via gel. The intensity of the F-tagged band at high concentrations of urea is assumed to correlate positively with the strength of the dimer.



## **DISCUSSION:**

### *Non-specific Binding to the Ni-NTA Resin:*

As noted above, the presence of each F-tagged triplet on the immunoblot following Ni-NTA purification is indirect evidence of dimerization with 7-9MH. The resin has no specific affinity for the F-tag. Furthermore, the primary sequences of each triplet receptor contain no internal polyhistidine regions<sup>14</sup>. Therefore, these triplets are likely interacting with 7-9MH itself, which does bind to the resin. This would be one explanation for why the triplet-F proteins were eluted from the resin alongside 7-9MH.

This conclusion is complicated somewhat by the unexpected presence of the two F-tagged proteins (1-3F and 7-9F) when no 7-9MH was present. Since Ni-NTA has no known affinity for either, their presence is most likely the result of non-specific resin binding. Preliminary experiments have shown that Myc-tagged triplets bind to the resin in isolation as well, so this hypothesis can be corroborated somewhat. At the very least, the F-tag is not the cause of this unexpected binding.

That said, are the triplet-F bands seen in the figures above the result of protein dimerization or non-specific binding? A definitive assessment cannot be made with the information available at this moment, so the results of this entire experiment are highly contentious. Modifications to the existing procedure may be made in the meantime to try and eliminate this non-specific binding issue. At present, there is an ongoing effort to block the Ni-NTA resin with a highly purified protein sample, such as ovalbumin (OVA), before the cell lysates are added. The purpose of this would be to minimize unintentional binding (similar to how one would block a membrane prior to immunoblotting). The results of this effort are not conclusive enough to be commented on yet, however. A second option worth exploring would be to increase the stringency of the Wash Buffer. Increasing the concentration of imidazole in the washes would potentially flush the non-specific proteins from the resin.

### *Insight into the Structure of the M6P/IGF2 Receptor:*

If one assumes that the effects of non-specific binding are negligible however, a host of conclusions can be drawn regarding the interaction of 7-9 with the other triplets. First, the relative amount of triplet-F protein still bound to 7-9MH following the disruption assay suggests that 7-9 dimerizes preferentially with certain triplet receptors over others. In particular, 7-9 shows the highest affinity for other 7-9 triplets. Interactions grow weaker as 7-9 pairs with triplets further away from itself, such as 1-3 and (presumably) 13-15. This pattern would indicate that proximity plays a role in dimerization.

This implies, further, that structure is the best predictor of dimerization strength. If two triplets are structurally identical (i.e. 7/9 and 7/9) then they will bind together best. Triplet receptor function is not as powerful an indicator. If it were, 7-9 would be expected to have a greater affinity for 1-3 since both bind extracellular M6P proteins. The nature of each interaction can be commented on as well. The disruption assays only succeeded when DTT (a reducing agent) was used. This suggests that a disulfide linkage is potentially holding the triplets together, in addition to any other non-covalent interactions that might be occurring.

### *Directives for Future Research:*

Naturally, there are limitations to each of the conclusions made above. For one, this study lacks information regarding the 13-15 triplet. Since this receptor did not express in appreciable quantities, one can only conjecture about its potential to dimerize with 7-9MH. Based on the trend

seen with the other four triplets, a weak interaction can be predicted; however, there is no data at present to support this claim. In addition, it is unknown whether the pattern observed with 7-9MH will hold true for the other triplets. Separate experiments would need to be done pairing the four remaining MH-triplets with the same F-tagged panel used here. Does proximity/structure influence the binding of each triplet pair, or just when 7-9 is examined? Of course, depending on the severity of the non-specific binding discussed above, all of these previous conclusions might be invalid anyway.

Once the entire length of the M6P/IGF2 receptor has been characterized, further experiments should strive to investigate how dimerization affects the receptor's ability to sequester ligands from the extracellular matrix. Thus, the work presented here is only a small fraction of a larger endeavor. Future experiments with the receptor may reveal something about its mechanism of tumor suppression that was previously unknown. This knowledge could then be applied toward cancer research at large.

**REFERENCES:**

- (1) Ghosh, P., Dahms, N. M., and Kornfeld, S. (2003) Mannose 6-phosphate receptors: new twists in the tale. *Nat Rev Mol Cell Biol* 4, 202-12.
- (2) Brown, J., Delaine, C., Zaccheo, O. J., Siebold, C., Gilbert, R. J., van Boxel, G., Denley, A., Wallace, J. C., Hassan, A. B., Forbes, B. E., and Jones, E. Y. (2008) Structure and functional analysis of the IGF-II/IGF2R interaction. *Embo J* 27, 265-76.
- (3) Linnell, J., Groeger, G., and Hassan, A. B. (2001) Real time kinetics of insulin-like growth factor II interaction with the IGF-II/mannose 6-phosphate receptor. *J. Biol. Chem.* 276, 23986-91.
- (4) Dahms, N. M. (1996) Insulin-like growth factor II/cation-independent mannose 6-phosphate receptor and lysosomal enzyme recognition. *Biochem Soc Trans* 24, 136-41.
- (5) Filson, A. J., Louvi, A., Efstratiadis, A., and Robertson, E. J. (1993) Rescue of the T-associated maternal effect in mice carrying null mutations in *Igf-2* and *Igf2r*, two reciprocally imprinted genes. *Development* 118, 731-6.
- (6) Brown, J., Delaine, C., Zaccheo, O. J., Siebold, C., Gilbert, R. J., van Boxel, G., Denley, A., Wallace, J. C., Hassan, A. B., Forbes, B. E., and Jones, E. Y. (2008) Structure and functional analysis of the IGF-II/IGF2R interaction. *EMBO* 27, 265-276.
- (7) Ludwig, T., Eggenschwiler, J., Fisher, P., D'Ercole, A. J., Davenport, M. L., and Efstratiadis, A. (1996) Mouse mutants lacking the type 2 IGF receptor (IGF2R) are rescued from perinatal lethality in *Igf2* and *Igf1r* null backgrounds. *Dev Biol* 177, 517-35.
- (8) Lau, M. M., Stewart, C. E., Liu, Z., Bhatt, H., Rotwein, P., and Stewart, C. L. (1994) Loss of the imprinted IGF2/cation-independent mannose 6-phosphate receptor results in fetal overgrowth and perinatal lethality. *Genes Dev* 8, 2953-63.
- (9) Martin-Kleiner, I., and Troselj, K. G. (2010) Mannose-6-phosphate/insulin-like growth factor 2 receptor (M6P/IGF2R) in carcinogenesis. *Cancer Lett.* 289, 11-22.
- (10) Byrd, J. C., and MacDonald, R. G. (2000) Mechanisms for high affinity mannose 6-phosphate ligand binding to the insulin-like growth factor II/mannose 6-phosphate receptor. *J Biol Chem* 275, 18638-46.
- (11) Byrd, J. C., Park, J. H., Schaffer, B. S., Garmroudi, F., and MacDonald, R. G. (2000) Dimerization of the insulin-like growth factor II/mannose 6-phosphate receptor. *J Biol Chem* 275, 18647-56.
- (12) Hartman, M. A., Kreiling, J. L., Byrd, J. C., and MacDonald, R. G. (2009) High-affinity ligand binding by wild-type/mutant heteromeric complexes of the mannose 6-phosphate/insulin-like growth factor II receptor. *Febs J* 276, 1915-29.
- (13) York, S. J., Arneson, L. S., Gregory, W. T., Dahms, N. M., and Kornfeld, S. (1999) The rate of internalization of the mannose 6-phosphate/insulin-like growth factor II receptor is enhanced by multivalent ligand binding. *J Biol Chem* 274, 1164-71.
- (14) Mungall, A. J., Palmer, S. A., Sims, S. K., Edwards, C. A., Ashurst, J. L., Wilming, L., Jones, M. C., Horton, R., Hunt, S. E., and Scott, C. E. (2003) The DNA sequence and analysis of human chromosome 6. *Nature* 425, 805-11.